

Conf-920792-61

Optical and infrared spectra of thermally annealed Pb implanted SiO_2 glasses

The submitted manuscript has been authored by a contractor of the U.S. Government under contract No. DE-AC05-84OR21400. Accordingly, the U.S. Government retains a nonexclusive, royalty-free license to publish or reproduce the published form of this contribution, or allow others to do so, for U.S. Government purposes.

D. O. Henderson, S. H. Morgan and R. Mu
Physics Department, Fisk University
Nashville, TN 37208

R. H. Magruder, III, and T. S. Anderson
Physics Department, Belmont University
Nashville, TN 37208

J. E. Wittig
Materials Science and Engineering Department
Vanderbilt University, Nashville, TN 37235

R. A. Zehr
Solid-State Division, Oak Ridge National Laboratory
Oak Ridge, TN 37831

ABSTRACT

Infrared reflectance between 4000 and 100 cm^{-1} and optical spectra between 1.8 and 6.2 eV of high purity silica implanted with nominal doses of 1, 3 and 6×10^{16} Pb ions/ cm^2 were recorded before and after annealing at 400, 600, and 800 °C for 1 hour. Curve resolution analysis of the Si-O stretching region resulted in six peaks which were characterized by their lineshape parameters. The oscillator strength of the ion induced defect peak at 1035 cm^{-1} was found to depend on ion dose. The defect band at 1035 cm^{-1} decreased to an intensity comparable to that of the unimplanted glass after thermal annealing for 1 hour at 800 °C. Far infrared spectra indicated the formation of lead silicate particles after annealing.

INTRODUCTION

The large polarizability of ions in a host glass makes them interesting candidates for all optical switching.¹ The nonlinear optical response arises from the nonresonant polarization of the ions and is strongly dependent on the host environment and the chemical state of the ion.² A low absorption index, a high damage threshold, and a sub-picosecond response are additional characteristics of this class of materials which are desirable for photonic devices. Bulk glasses containing lead ions have been considered as potential candidates for photonic applications. However, the processing and the mode of formation of these bulk glasses are not always compatible with current technology used for waveguides and other photonic devices.

Ion implantation is another method for incorporating polarizable ions in a substrate and allows for precise control of the concentration and thickness of the layer. In addition new nonequilibrium phases can be created which are not constrained by chemistry or equilibrium thermodynamics. This technology is particularly attractive for optical device fabrication as it is compatible with present semiconductor and waveguide technology.

In this paper we report the infrared, optical, and TEM measurements for Pb implanted silica before and after the annealing cycles. The ion dose and thermal annealing dependence of the Si-O stretching peak was analyzed by nonlinear curve resolution techniques.

MASTER

SP

DISTRIBUTION OF THIS DOCUMENT IS UNLIMITED

Henderson

EXPERIMENTAL

Spectrosil A substrates, 2.0 cm in diameter and 0.1 cm thick were implanted with Pb^{++} ions at an energy of 320 keV and with a flux of $2.6\mu\text{amps}/\text{cm}^2$. Ion backscattering with 2 MeV He^+ ions were used to measure the depth profile for all doses. Implantations and backscattering measurements were done at Oak Ridge National Laboratory.

Samples for transmission electron microscopy were prepared by cutting 3mm diameter discs from the implanted wafers with a slurry drill, mechanically grinding the disc from the backside to a thickness of $100\mu\text{m}$, and dimple grinding to approximately $20\mu\text{m}$ from the implanted surface. Final thinning to electron transparency was achieved by backthinning with a single Ar gun at 6 keV. To minimize ion damage, the samples were cryogenically cooled during ion milling. These samples were examined in a Philips CM20/T scanning electron microscope operating at 200 keV. Standard bright field imaging and selected area electron diffraction were used to characterize the implanted layer of the silica wafers. The samples were carbon coated to eliminate charging effects.

Optical absorption measurements were made at room temperature from 650 to 200 nm (1.8 to 6.2 eV) using a Cary 14 dual beam spectrometer interfaced with a data acquisition system. All samples were measured using an unimplanted sample in the reference beam. Hence all absorption measurements shown are the difference between the implanted and unimplanted glasses. The spectra are reported as a function of absorption per implanted ion, i.e. extinction coefficient. The absorption spectra were measured at three different positions on each sample. The scatter in the extinction coefficient due to these positions is less than 5%. Samples implanted at 1 and 6×10^{16} ions/ cm^2 were thermally annealed in air at 400, 600, and 800°C for 1 hour. The absorption spectra were measured after each annealing treatment.

A laboratory built reflectance accessory adjusted to an angle of incidence of 25° was used for the infrared reflectance measurements. Reflectance spectra between 800 and 100 cm^{-1} were recorded with a Bomem DA3.02 FTIR spectrometer and the region between 4000 and 400 cm^{-1} were measured with a Bomem MB-100 FTIR spectrometer. All spectra were recorded at 4 cm^{-1} resolution and a gold mirror was used as reference. The spectra of the as-implanted and annealed samples were normalized against the gold mirror to provide consistency in the measurement. Repeated measurements on the samples established that the intensities and the frequencies in the reflectance spectra were reproducible to $+/- 0.5\%R$ and $+/- 0.4\% \text{cm}^{-1}$, respectively.

RESULTS

Figure 1 shows the RBS data for the Pb implanted silica. For all doses the line profiles are Gaussian. All implanted ion doses as measured by RBS were generally $>85\%$ the nominal implantation dose.

Standard bright field imaging techniques were used to characterize the ion implanted layer. Electron diffraction patterns from the sample implanted with a dose of 6×10^{16} ions/ cm^2 display a polycrystalline ring pattern, characteristic of a face centered cubic metallic crystal structure, superimposed on the diffuse diffracted intensity from the amorphous silica matrix. Figures 2 and 3 show the micrographs for samples implanted with doses of 3 and 6×10^{16} ions/ cm^2 . The particles are irregular in shape. The size of the particles range from 2 to 10 nm in diameter.

DISCLAIMER

This report was prepared as an account of work sponsored by an agency of the United States Government. Neither the United States Government nor any agency thereof, nor any of their employees, makes any warranty, express or implied, or assumes any legal liability or responsibility for the accuracy, completeness, or usefulness of any information, apparatus, product, or process disclosed, or represents that its use would not infringe privately owned rights. Reference herein to any specific commercial product, process, or service by trade name, trademark, manufacturer, or otherwise does not necessarily constitute or imply its endorsement, recommendation, or favoring by the United States Government or any agency thereof. The views and opinions of authors expressed herein do not necessarily state or reflect those of the United States Government or any agency thereof.

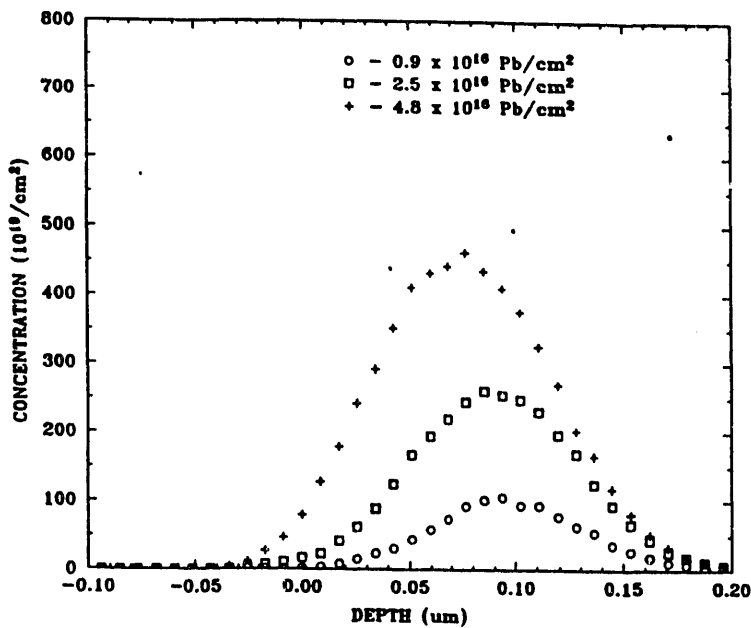


Figure 1. Profile of Pb ion concentration as a function of distance from the surface.

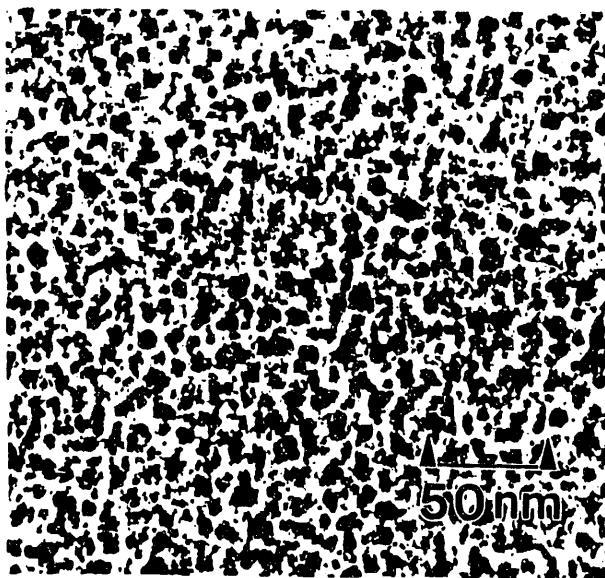


Figure 2. Bright-field TEM images of Pb implanted layers for sample implanted with 3×10^{16} ions/cm 2 .

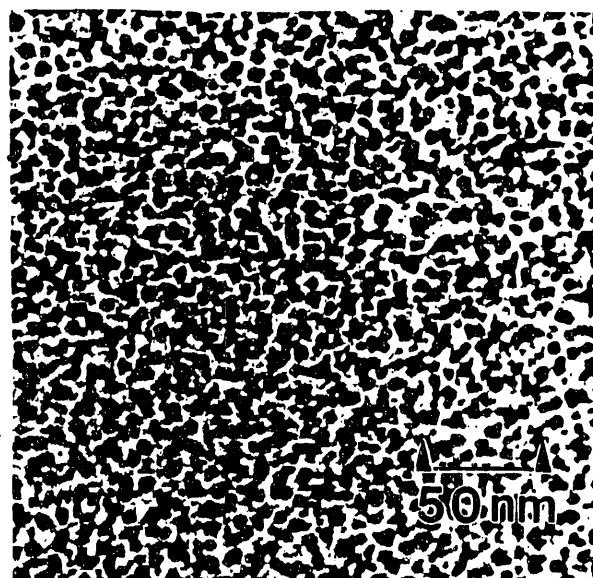


Figure 3. Bright field TEM images of Pb implanted layers for sample implanted with 6×10^{16} ions/cm 2 .

In figure 4, the optical absorption as a function of photon energy is shown for three samples. Absorption increases from 1.8 to 5.4 eV with a resolved but broad peak near 5.2 eV for the sample implanted with a dose of 1×10^{16} ions/cm 2 . Similar behavior is observed in the other samples except the peak near 5.2 eV becomes a broad shoulder that increases in magnitude with increasing dose as does the absorption throughout the rest of the region of the measurement.

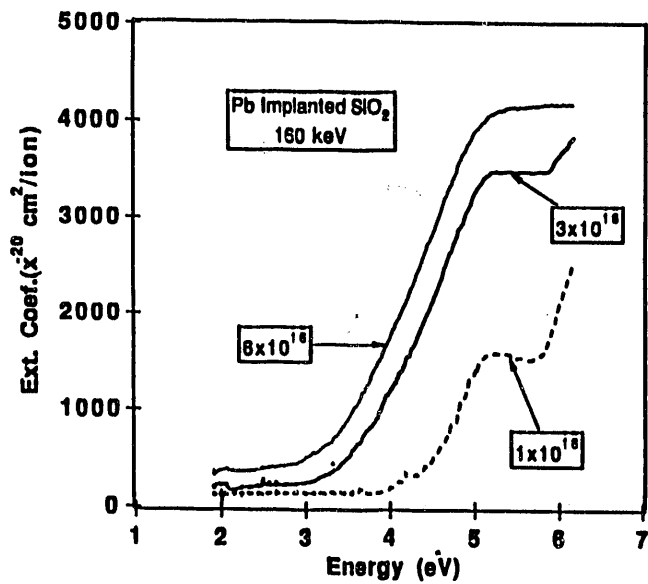


Figure 4. Optical absorption as a function of energy.

In figure 5 the absorption spectra for the sample implanted with 6×10^{16} ions/cm² is shown after annealing at 800°C for 1 hour. There were no changes observed outside of error in the optical absorption for the samples annealed at 400 and 600°C. The difference spectra are also included in the figure. The difference spectra shows that peaks at ~4.8 eV and at ~5.8 eV are annealed out. Figure 6 shows the absorption spectra for the sample implanted with a dose of 1×10^{16} ions/cm² as implanted, after annealing at 800°C and the their difference spectra. The peaks which show anneal out are the same as for those in the 6×10^{16} ions/cm² sample.

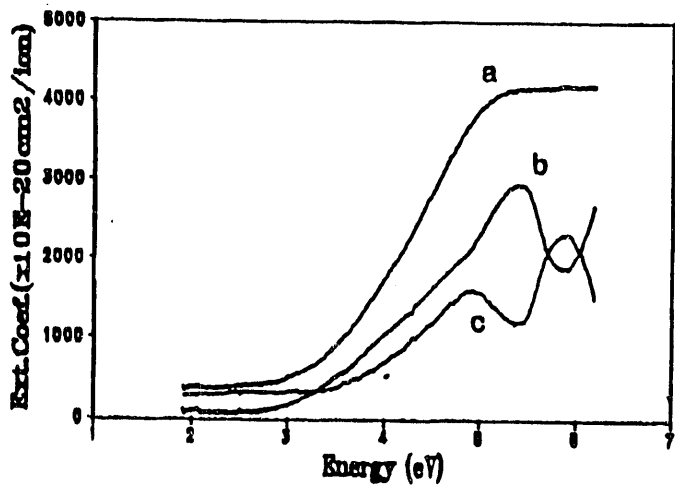


Figure 5. Optical absorption as a function of energy for sample implanted with 6×10^{16} ions/cm² a) as implanted, b) after 800°C anneal, c) difference spectra.

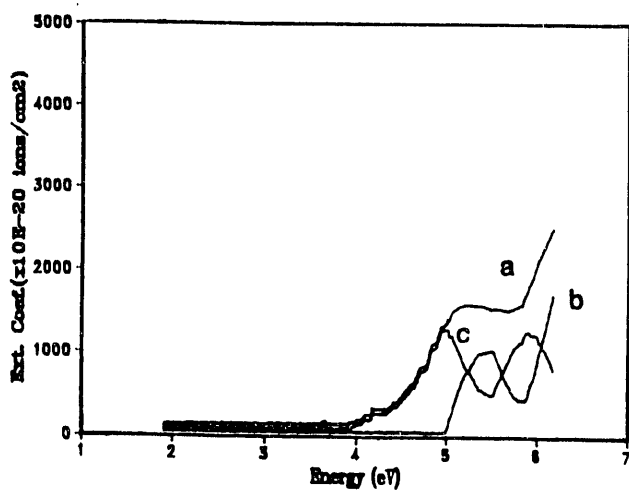


Figure 6. Optical absorption as a function of energy for sample implanted with 3×10^{16} ions/cm² a) as implanted, b) after 800°C anneal, c) difference spectra.

Representative spectra of the Si-O stretching region for unannealed samples implanted with 1, 3, and 6×10^{16} ions/cm² together with an unimplanted sample are shown in figure 7. The most intense feature in these spectra is the peak near 1117 cm⁻¹ which we assign to the TO mode and the higher frequency component at 1220 cm⁻¹ to the LO mode.³ The peak near 1035 cm⁻¹ is assigned to the dangling bond Si-O stretching vibration.⁴ Spectra for the same region for sample dosed with 6×10^{16} ions/cm² and annealed at 400, 600, and 800°C are shown in figure 8. Assignments for the peak maxima in the annealed samples are the same as that given for the as-implanted samples.

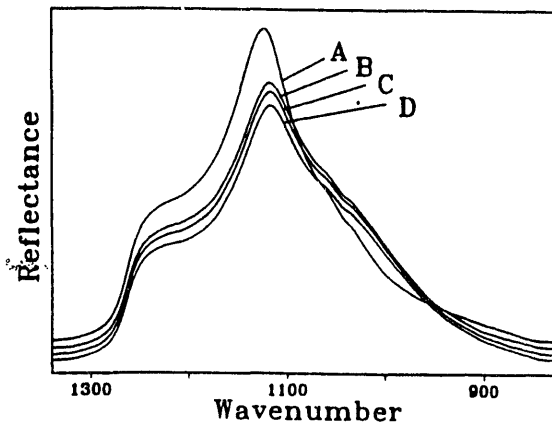


Figure 7. Infrared reflectance spectra of the ion dose effect on Si-O stretch vibrations of Spectrosil A samples. a) Unimplanted, b) ion dose of 1×10^{16} , c) ion dose of 3×10^{16} , d) ion dose of 6×10^{16} .

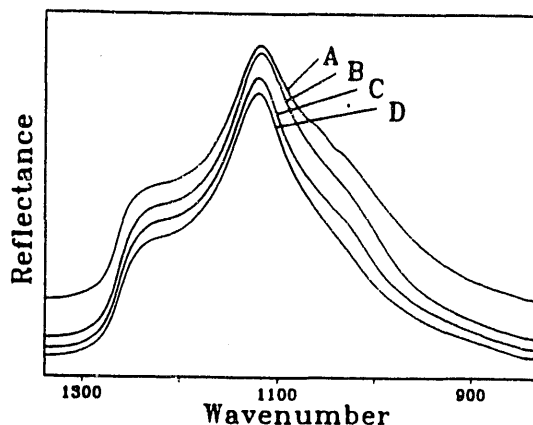


Figure 8. Infrared reflectance spectra of the thermal treatment effect on ion implanted Spectrosil A with the dose of 6×10^{16} ions/cm². a) As-implanted, b) thermally annealed at 400°C, c) thermally annealed at 600°C, d) thermally annealed at 800°C.

The curve fitting was performed using the Levenberg-Marquardt algorithm.⁵ Initial parameters for the band centroid, height, FWHH and Lorentz fraction are required to begin the least squares optimization. All line shape parameters were unconstrained and allowed to vary in the optimization. A total of six component bands were required to reproduce the experimental spectrum. Additional components did not significantly decrease the residual. Results for the curvefit are shown in figure 9 for the as-implanted and the 800°C annealed sample with a dose of 6×10^{16} ions/cm².

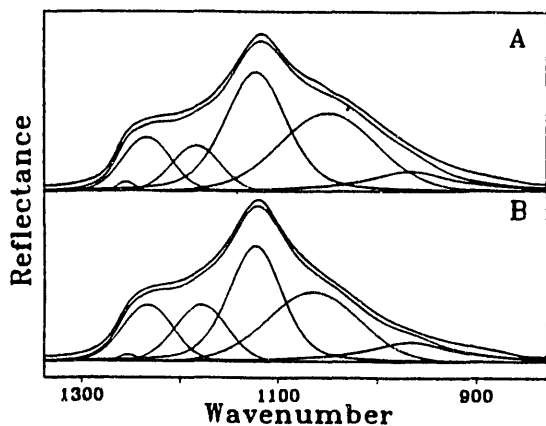


Figure 9. Curve fits for the SiO stretching region for a) as implanted and b) annealed at 800°C for an ion dose of 6×10^{16} ions/cm².

Of the six component bands obtained from the curve fit, only the 1126 and 1057 cm^{-1} components changed significantly with ion dose and the annealing cycles. Their dependence on ion dose and annealing temperature are shown in figures 10 and 11. The intensities and the line widths for 1126 and 1057 cm^{-1} components are sensitive to the dose and annealing while the other components appear to independent of dose and the annealing cycles. The intensity of 1050 cm^{-1} band for the 1, 3 and 6×10^{16} ions/ cm^2 samples increases as the ion dose increases, while the intensity of the 1126 cm^{-1} decreases with ion dose. Annealing these samples reverses the trend, i.e. the 1126 cm^{-1} peak increases after annealing and the 1050 cm^{-1} component decreases in intensity upon annealing. Both bands show increases in line width as the ion dose increases and both decrease after annealing.

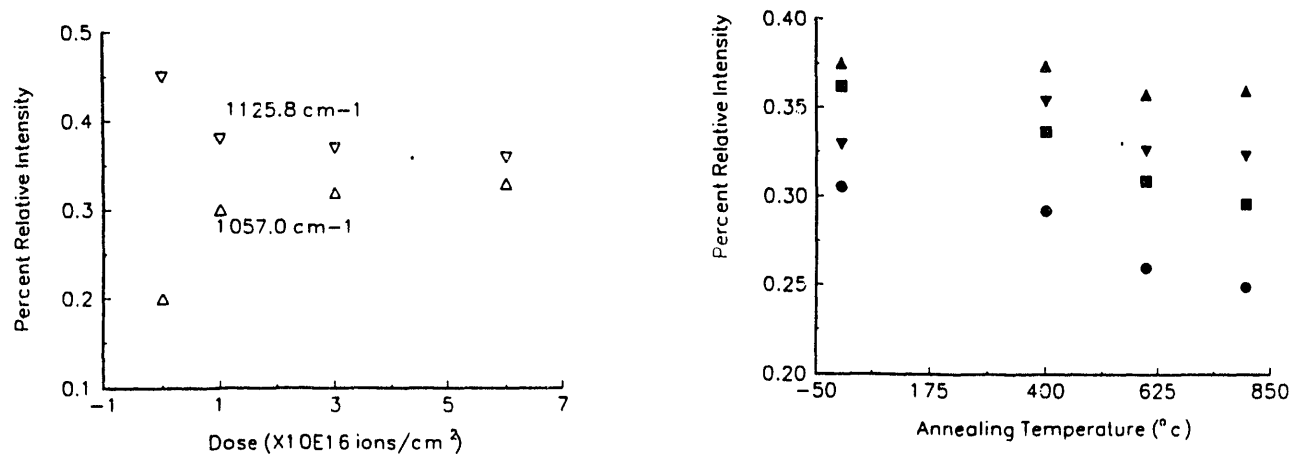


Figure 10. Ion dose and thermal annealing effects on the vibrational intensity of Si-O stretch of TO mode at 1125.8 cm^{-1} and on the dangling bond Si-O stretch at 1057 cm^{-1} . (left) Dose effect. (right) Thermal annealing effect. (symbols: triangle up (1125.8 cm^{-1} , 1×10^{16}), triangle down (1125.8 cm^{-1} , 6×10^{16}), square (1057 cm^{-1} , 6×10^{16}), and circle (1057 cm^{-1} , 1×10^{16})).

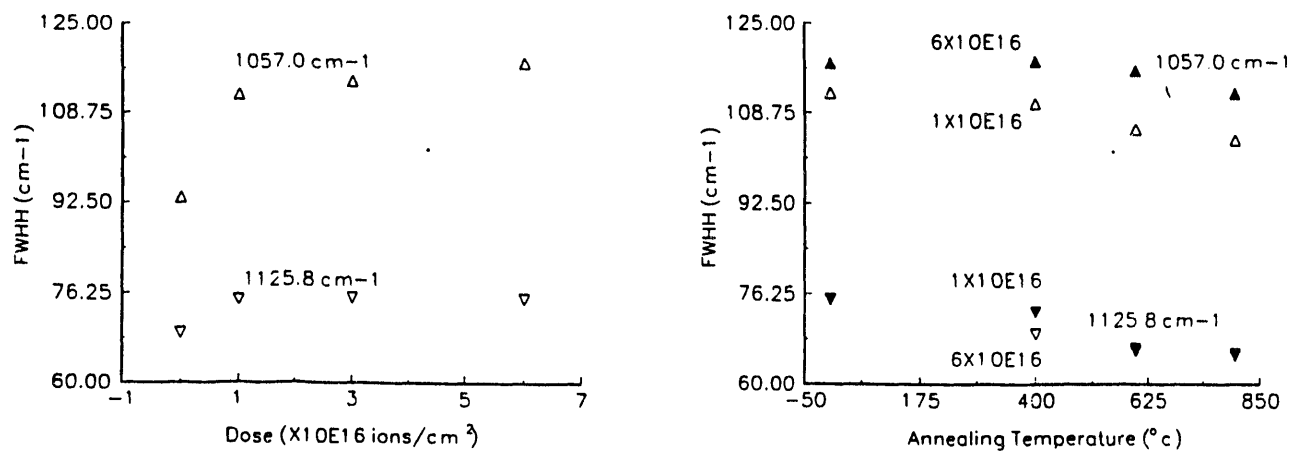


Figure 11. Ion dose and thermal annealing effects on the band width (FWHH: full width at half height) of TO mode and dangling bond of Si-O stretch. (left) Ion dose effect. (right) Thermal annealing effect.

Far infrared spectra for the 6×10^{16} ions/cm² sample after annealing together with a bulk glass (30PbO70SiO₂) are shown in figure 12. Reflectance maxima are observed at 221 and 148 cm⁻¹ which are not present in the unimplanted sample. These peaks are assigned the Pb-O stretching mode of covalent and ionic bonded PbO.⁶ Annealing the sample results in broadening the peaks.

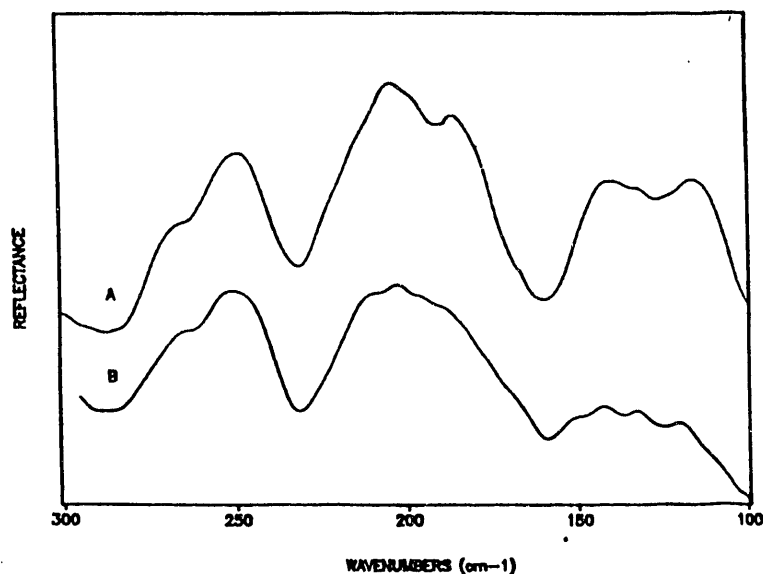


Figure 12. Far infrared spectra of the Pb-O stretching region for a) a bulk lead silicate glass (30PbO70SiO₂) and b) the 800°C annealed sample with a dose of 6×10^{16} ions/cm².

DISCUSSION

The electron diffraction patterns clearly show the formation of small metallic lead particles. The density of these particles increase with increasing dose. There was no evidence of metallic level in the 1×10^{16} ions/cm² sample.

We attribute the changes in the optical absorption spectra to two sources. The first is due to defects caused by implantation damage. Ion implantation is known to produce E", B₂, and homobond defects with absorptions at 5, 5.8, and 7.6 eV. These defects are present and contribute to the absorption in the 5 to 6 eV region. We attribute the absorption at energies greater than 5.5 eV primarily to these defects. As the absorption is reported in terms of absorption per ion, the higher dose sample demonstrates that each ion produces a greater effect. Therefore we conclude that there is greater than 1 to 1 correspondence between implanted ion and defects. Based on oscillator strengths of E' and B₂ centers the magnitude of defects required to produce this absorption would require concentrations greater than ~ 50% of the Si-O sites.^{7,8} We conclude these defects cannot alone account for the magnitude of the absorption of the feature at 5.2 eV nor the change observed with increasing dose.

The second source is due to the presence of Pb ions. We attribute the broad peak and shoulder at 5.2 eV to the Pb ions. Parke and Webb,⁹ Stroud and Lell¹⁰ and Paul¹¹ have reported the absorption spectra for various silicate glasses containing a range of lead concentrations. They attribute the absorption in the 5.1-5.5 eV range to transitions for the Pb²⁺ ion. The position of this peak was observed to shift with the basicity of the glass suggesting that the local electronic structure affects the peak position. Based on these reports we attribute part of the absorption at 5.2 eV in our samples to the Pb²⁺ ion. The absorption reported as extinction coefficient shows a strong deviation from Beer's Law. The change in the extinction coefficient is interpreted in terms of a change in the way the implanted ion interacts with the host substrate with increasing dose. The breadth of this absorption peak may be partially due to the presence of different local environments in the glass structure and different degrees of covalent vs. ionic bonding as will be discussed below.

Part of the absorption throughout the spectral region examined is due to the presence of the PS metal particles. The theory of optical extinction due to metal particles in a dielectric was first put forth by Mie.¹² For small particles (radius $<\lambda/20$), the extinction is due to only absorption α and can be expressed as¹³:

$$\alpha = \frac{18\pi p n_d^3}{\lambda} \frac{\epsilon_2}{(\epsilon_1 + 2n_d^2) + \epsilon_2^2}$$

Where the dielectric constant of the metal is $\epsilon = \epsilon_1 + i\epsilon_2$, p is the volume fraction of metal and n_d is the index of refraction of the dielectric. The lead particles in our samples all have a radius $<\lambda/20$. The absorption will exhibit a maximum where $\epsilon_1 + 2n_d^2 = 0$. This is the condition for the surface plasmon resonance. For lead particles this is expected to occur ~ 6 eV however, in silica using the formalism of Doyle¹¹ we calculate that the absorption due to the surface plasmon resonance started to occur at ~ 3.5 eV. Other factors such as surface roughness, particle agereation and particle shape can cause shift in the position of this peak. These factors are reviewed in depth by Kreibis and Genzel.¹⁴ We do not observe a feature that can be definitely assigned to the surface plasmon resonance of the Pb particles. However, we do observe a general increase in absorption with increasing dose and we attribute this to an increase in p the volume fraction of metal with increasing dose. If the surface plasmon resonance exists we speculate that it is overlapped by the broad spectral features and Pb²⁺ ions. In addition as the Pb ions are distributed into different chemical states, the surface plasmon resonance may be small. Similar behavior with ion implantations of Fe in silica has been observed by Perez et al.¹⁵ The relative fraction of chemical states of Fe⁰, Fe²⁺ and Fe³⁺ were dose dependent.

We suggest that the annealing at 800°C causes the Pb clusters to dissolve and the Pb reacts with the silica to form a Pb-silicate phase as observed in melt prepared Pb silicates. The formation of this phase is seen in IR measurements.

The dose dependent changes in Si-O stretching region in the infrared reflectance spectra are attributed to the rupture of Si-O-Si linkages and the concomitant formation of dangling bonds. As shown in figure 10, the decrease in the intensity of the TO mode at 1126 cm⁻¹ tracks with the increase of the Si-O dangling bond peak at 1057 cm⁻¹ in a quantitative way. However, after a dose of 1×10^{16} ions/cm² the change in the intensity of these bands is relatively small and appears to saturate. Therefore it may be concluded that $\sim 85\%$ of the bond rupture occurs with the lowest dose. The affect of annealing the samples reverses the process. As the samples are annealed at 400, 600 and 800°C, the 1057 cm⁻¹ peak progressively decreases in intensity while the 1126 cm⁻¹ band increases. This trend we attribute to the reforming of Si-O linkages and therefore a loss of Si-O dangling bonds.

The ion dose induced increase of the linewidths for the 1126 and 1057 cm⁻¹ bands shown in figure 11 are attributed to a local perturbation to the SiO₄ tetrahedra due the presence of the Pb²⁺ ion and the formation of dangling bonds which may be altered by lead ions. Evidence for this perturbation can be seen from the far infrared spectra where absorptions due to the Pb-O stretching vibrations for covalent and ionic PbO are observed. The presence of these two types of bonding could contribute to the broadening of the peaks assigned to the TO and Si-O dangling bond modes. After annealing the sample, the peaks assigned to the Pb-O stretching vibrations broaden and are very close in frequency and width to a bulk lead silicate glass formed from the melt. In view of these observations, we conclude that annealing the lead implanted glass results in reforming the Si-O-Si linkages and the formation of a lead silicate phase.

CONCLUSIONS

The infrared spectra show that Pb-ion implantation in fused silica results in the rupture of Si-O-Si linkages and therefore also the creation of Si-O dangling bonds. The dose dependence and annealing were

analyzed quantitatively by curve resolution. Annealing the sample has two effects: 1) the formation of a lead silicate phase and 2) the reformation of Si-O-Si linkages.

The optical absorption spectra show that ion implantation produces defect peaks between 5.1 and 5.5 eV. Part of the absorption is attributed to the Pb²⁺ ion. The defect peaks disappear after annealing. A more refined control of the annealing process and implantation parameters could lead tailoring ion implanted glasses with properties more closely optimized for nonlinear optical devices. Characterization of ion implanted glass by infrared spectroscopy together with curve resolution analysis, optical absorption spectroscopy and TEM should serve as a feed back for aiding in refining implantation conditions and thermal and possibly laser annealing of ion implanted samples.

ACKNOWLEDGEMENT

The work at Belmont University was supported by the Research Corporation (RHM and TAA). The work at Fisk University was supported by NASA under the Fisk University Center for Photonic Materials and Devices (SHM) and by the Federal Aviation Administration (DOH). The work at Oak Ridge National Laboratories was supported by the Division of Materials Science, U.S. Department of Energy under contract DI-AC05-84OR21400 with Martin-Marietta Energy Systems, Inc.

REFERENCES

1. S. R. Friberg and P. W. Smith, IEEE J. Quantum Electronics, QE-23 (1987) 2089-2094. Nonlinear Optical Glasses for Ultrafast Optical Switching.
2. M. E. Lines, J. Appl. Phys., 69 (1991) 6876-6884 Oxide Glasses for Fast Photonic Switching: A Comparative Study.
3. F. L. Galeener and G. Lucovsky, Phys. Rev. Lett., 37 (1976) 1474-1478, Longitudinal Optical Vibrations in Glasses: GeO₂ and SiO₂.
4. R. H. Magruder, III, R.F. Haglund, S. H. Morgan, D. O. Henderson, R. A. Weller, L. Yang, and R. A. Zuhr, Nucl. Inst. and Methods B65 (1992) 405-411, Nonlinear Index of Refraction of Cu and Pb Implanted Fused Siliica.
5. W. H. Press, B. P. Flannery, S. A. Teukolsky, and W. T. Vetterling, "Numerical Recipes: The Art of Scientific Computing" Cambridge University Press, 1989).
6. T. Furukawa, S. A. Brawer, and W. B. White, J. of Materials Science, 13 (1978) 268-282, The Structure of lead Silicate Glasses by Vibrational Spectroscopy.
7. R. A. Weeks and E. Sonder in Paramagnetic Resonance; W. Low Ed. Academic Press, New York (1963) 869-879.
8. R. A. Weeks "Optical and Magnetic Properties of Ion Implanted Glasses", Materials Science and Technology vol. 9, J. Zarzychi, Ed. Weinheim (1991) 331-373
9. S. Parke and R. S. Webb, Phys. Chem. Solids, 34 (1973) 85-95, The optical Properties Thallium, Lead and Bismuth in Oxide Glasses.
10. J. S. Stroud and E. Lell, J. Am. Cer. Soc., 54 (1974) 554-555, Optical Absorption of Lead in Glass.
11. A. Paul, Phys. and Chem. of Glasses, 11 (1970) 46-52, Ultraviolet Absorption of Divalent Lead in Some Simple Glasses.
12. G. Mie Ann. Phys. 25 (1908) 377.
13. C. F. Bohren and D. R. Huffman, Absorption and Scattering of Light by Small Particles, John Wiley and Sons, New York, 1983.
14. U. Kreibig and L. Genzel, "Optical Absorption of Small Metallic Particles" Surface Science, 156 (1985) 678-700.
15. A. Perez, M. Treilleux, T. Capra, and G. Griscom, J. Mater. Res., 2 (1987) 910-917, Precipitation Phenomena in High Dose Iron Implanted Silica and Annealing Behavior.

**DATE
FILMED**

8 / 17 / 93

END

